PERGAMON

International Journal of Heat and Mass Transfer 44 (2001) 3111–3123

International Journal of HEAT and MASS TRANSFER

www.elsevier.com/locate/ijhmt

Tree-shaped insulated designs for the uniform distribution of hot water over an area

W. Wechsatol [a], S. Lorente [b], A. Bejan [a,*]

[a] *Department of Mechanical Engineering and Materials Science, Duke University, Box 90300, Durham, NC 27708-0300, USA*
[b] *Department of Civil Engineering, National Institute of Applied Science (INSA), 135 Avenue de Rangueil, Toulouse 31077, France*

Received 13 September 2000; received in revised form 9 October 2000

Abstract

This paper is a study of the optimal geometric layout of schemes for distributing hot water uniformly over an area. Constrained are the amount of insulation material, the volume of all the pipes, and the amount of pipe wall material. Unknown are the distribution of insulation over all the links of the network, and the configuration of the network itself. The main focus is on how the geometric configuration may be selected in the pursuit of maximized global performance, and how closely a non-optimal configuration performs to the highest level. Three global optimization criteria are considered, and they all yield similar results with respect to the distribution of insulation: the maximization of the temperature of the hot water received by the farthest user, the minimization of the total heat loss of the network, and the maximization of the delivery temperature averaged over all the users. Three configurations are optimized: (a) an area covered by a coiled stream, where all the users are aligned on the same stream, (b) a sequence of tree-shaped flows on square areas in which each area construct is made up of four smaller area constructs, and (c) a sequence of tree-shaped flows where each area construct is made up of two smaller area constructs. It is shown that the tree-shaped designs (b) and (c) outperform consistently and significantly the coiled stream design (a). The tree designs obtained by pairing (c) are better than the square tree constructs (b) and, in addition, they deliver water at the same temperature to all the users spread over the territory. The optimized tree networks (b) and (c) approach the same high level of global performance as their complexity increases. Optimized tree-shaped flow designs are robust.

Keywords: Topology optimization; Tree networks; Dendritic; Constructal; Hot water distribution; Insulation; Flow resistance minimization

1. Configuration optimized, not frozen

The usual method of modeling, analysis and optimization in thermal engineering begins with assuming the system configuration – its geometry, architecture, components and manner in which the components are connected. Next, the model that is conceived is a simplified facsimile of the assumed system, while the analysis is the mathematical description of the model and its performance. The optimization is the simulation of system operation under various conditions, and the search for the operating conditions most favorable for achieving maximum performance.

The search for optimal design is considerably more challenging than optimizing the operation of a single (assumed) configuration. In principle, one may contemplate a very large number of possible geometric configurations, all the way to large numbers of duct shapes and aspect ratios in every detail of a fluid flow network. In practice, one may consider one or two alternative configurations, optimize their performance as in the preceding paragraph, and compare in the end the optimized alternatives. Selecting the best among two or three is to optimize the design. Important to the

* Corresponding author. Tel.: +1-919-660-5310; fax: +1-919-660-8963.
E-mail address: abejan@duke.edu (A. Bejan).

0017-9310/01/$ - see front matter
PII: S0017-9310(00)00338-0

Nomenclature

A	area (m^2)
A_i	area covered by the construct of level i (m^2)
c_1, c_2, c_2', c_3, c_4	constants, Eqs. (9), (16), (17), (20) and (23)
c_p	specific heat at constant pressure (J/kg K)
D	diameter of round territory, Fig. 1 (m)
f	friction factor
I_1, I_2, I_3, I_4	integrals, Eqs. (7), (8), (13) and (15)
k	thermal conductivity (W/m K)
L	length (m)
L_0	elemental length (m)
$\dot{m}$	mass flow rate (kg/s)
$\dot{m}_i$	initial mass flow rate (kg/s)
n	exponent, Eq. (17)
N	number of heat loss units, Eq. (5)
N_0	elemental number of heat loss units, Eq. (28)
q	heat transfer rate (W)
$\tilde{q}$	dimensionless heat transfer rate, Eq. (19)
q'	heat transfer rate per unit length (W/m)
r_i	inner radius of insulation (m)
r_{i0}	smallest r_i size available (m)
r_0	outer radius of insulation (m)
R	ratio of insulation annulus radii, r_0/r_i
S	side of square territory, Fig. 1 (m)
T	temperature (K)
$\overline{T}$	temperature averaged over all the users (K)
$\tilde{T}$	dimensionless temperature, Eq. (21)
T_0, T_{end}	end user temperature (K)
T_∞	ambient temperature (K)
V	volume of insulation material (m^3)
$\tilde{V}$	dimensionless insulation volume, Eqs. (35) and (40)
V_p	volume of pipe wall material (m^3)
$\dot{W}_0$	pumping power (W)
x	longitudinal position (m)
z	depth (m)

Greek symbols

β	dimensionless notation, $(r_{i1}/r_{i0})^2$
ΔP	pressure drop (Pa)
θ	dimensionless temperature, Eqs. (34) and (39)
ξ	dimensionless longitudinal position, x/L
ρ	density (kg/m^3)

Subscripts

i	level of construct, or assembly
max	maximum
opt	optimum
$0, 1, 2, \ldots$	elemental, first construct, second construct, ….(1)

subject of this paper is that comparing the optimized candidates represents the optimization of geometric configuration, which was allowed to vary.

Configuration (geometry, topology) is the chief unknown and major challenge in design. The case-by-case choices that we are accustomed to making are educated guesses. Better designers make choices that work, i.e., configurations that have been tested. Experience and longevity are useful when the needed system is envisioned as an assembly of already existing parts. Is this the way to proceed in every application? It would be useful to the designer to have access from the beginning to the infinity of configurations that exist. Access means freedom to contemplate them all, without constraints based on past experience. It would also be useful to have a strategy (route, guide) to which architectural features lead to more promising configurations, and ultimately to better optimized designs.

The objective of this paper is to illustrate this approach to flow system design, specifically, the view that configuration itself is the unknown to be optimized [1]. We do this by considering the fundamental problem of distributing a supply of hot water as uniformly as possible over a given territory. This is a classical problem of civil engineering, with related subfields in piping networks, sewage and water runoff, irrigation, steam piping, etc. [2–5]. Recent studies of hot water distribution networks are [6–9]. For example, unlike in [8], where the flow path geometry is assumed and frozen throughout the remaining optimization process, in the present study we reserve the freedom to change the configuration, to "morph" it into better patterns en route to higher levels of performance.

The present treatment of the hot water distribution problem is restricted to its thermo-fluid aspects. Considerations of insulation cost [10] and exergetic costs associated with capital and flow irreversibilities [11] are left for more advanced models that could be subjected to the approach outlined in this article. The distribution of hot water to users on a specified territory presents two problems to the thermal designer: the fluid mechanics problem of minimizing the pumping power, and the heat transfer problem of minimizing the loss of heat from the piping network. The water flow is from one point (the source) to an area – the large number of users spread uniformly over the area.

The fluid mechanics problem has been addressed in various forms, not only in engineering [1,2] but also in physics and biology [12–23]. The addition of the heat transfer problem in this paper is new, especially on the background of the existing work on tree-shaped flows of heat from point to area, or point to volume [1]. The heat trees that have been optimized geometrically until now were generated by the requirement to minimize the global thermal resistance encountered by the point-volume heat current. In the present heat transfer problem the requirement is just the opposite. It is to prevent the flow of heat from the branches of the piping network to the area (the 'ambient'). This is to be accomplished by using a specified (finite) amount of thermal insulation for all the pipes, and by distributing it optimally.

2. Elemental string of users

The area A is supplied with hot water by a stream of flow rate $\dot{m}$ and initial temperature T_i. The stream enters the area from the outside, by crossing one of its boundaries. The area is inhabited by a large number of users, $n = A/A_0$, where A_0 is the area element allocated to a single user. Let A_0 be a square with the side length L_0, so that A constitutes a patch work of n squares of size A_0. Each elemental square must receive an equal share of the original stream of hot water, $\dot{m}/n$. As in all the point-area tree flows considered previously [1], the fundamental question is how to connect the elements so that the ensemble (A) performs best.

We begin with the simple option of supplying a large number of elements with the same stream, which is a straight or curved line of length L (Fig. 1). The initial (entering) flow rate is $\dot{m}_i$ The flow rate $\dot{m}(x)$ decreases linearly to $\dot{m}(0) = 0$, because each user draws the same share of $\dot{m}_i$ per unit length x. It is assumed that the number of elements is sufficiently large so that the variation of $\dot{m}(x)$ may be treated as continuous

$$\dot{m}(x) = \frac{x}{L}\dot{m}_i. \tag{1}$$

The temperature of the stream $T(x)$, decreases from its original temperature T_i (at $x = L$) because of the leakage of heat to the ambient. We assume that the dominant thermal resistance between the stream and the ambient is posed by a cylindrical shell of thermal insulation installed on the outside of the pipe that carries the stream. In this limit the rate of heat loss per unit of pipe length is [24]

$$q' = \frac{2\pi k}{\ln(r_0/r_i)}[T(x) - T_\infty], \tag{2}$$

where r_0, r_i, k and T_∞ are the outer and inner radii of the insulation, the thermal conductivity of the insulating material, and the ambient temperature. Written for a pipe length $\mathrm{d}x$, the first law of thermodynamics requires

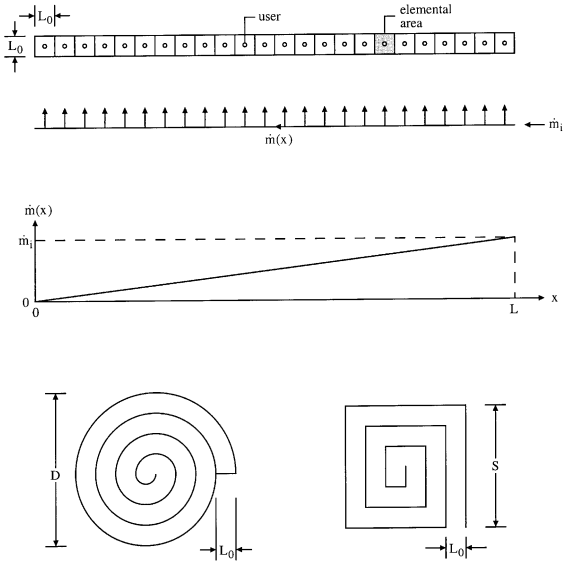

Fig. 1. String of users supplied by a single stream of hot water, and round and square areas served by the string-shaped stream.

$$\dot{m}c_p\,\mathrm{d}T = \frac{2\pi k}{\ln(r_0/r_i)}(T - T_\infty)\,\mathrm{d}x. \tag{3}$$

The temperature distribution along the water stream (or the pipe wall) is obtained by integrating Eq. (3) from $x = L$ where $T = T_i$

$$\frac{T(x) - T_\infty}{T_i - T_\infty} = \exp\left(-N\int_x^L \frac{\mathrm{d}x}{x\ln(r_0/r_i)}\right), \tag{4}$$

where, by analogy with the number of heat transfer units defined for heat exchangers, N is the "number of heat loss units" of the L-long pipe system

$$N = 2\pi kL/\left(\dot{m}_i c_p\right). \tag{5}$$

The temperature of the hot water delivered to the users is $T(x)$: according to Eq. (4), this is known as soon as the distribution of thermal insulation is known, namely, the ratio r_0/r_i as a function of x. The constraint is the total amount of insulation wrapped around the pipe

$$V = \pi\int_0^L \left(r_0^2 - r_i^2\right)\mathrm{d}x. \tag{6}$$

3. Optimal pipe radius

The geometry of the pipe and its insulation is described completely by r_0 and r_i (or r_0/r_i and r_i) as functions of x. The optimal distribution of pipe size

$[r_i(x)]$ can be derived from the minimization of the pumping power $\dot{W}$ required to drive $\dot{m}(x)$ through the entire system. The pumping power varies as the product $\dot{m}(\mathrm{d}P/\mathrm{d}x)$, while in fully rough turbulent flow the pressure gradient is proportional to $\dot{m}^2/r_i^5$. In conclusion, the pumping power per unit length varies as $\dot{m}^3/r_i^5$, or x^3/r_i^5, and the objective is to minimize the integral

$$I_1 = \int_0^L \frac{x^3}{r_i^5}\,\mathrm{d}x. \tag{7}$$

If the constraint is the pipe wall material, then the pipe size must vary such that the integral

$$I_2 = \int_0^L r_i\,\mathrm{d}x \tag{8}$$

remains fixed. Specifically $I_2 = V_p/(2\pi t)$, where V_p is the volume of the pipe-wall material, and t is the wall thickness, which is assumed considerably smaller than r_i. The same constraint applies when fixed is the volume of excavated soil that is required for burying the pipe system to a constant depth z. In that case I_2 scales as $V_s/(2z)$, where V_s is the volume of excavated soil.

The variational calculus [25] solution to the problem of minimizing I_1 subject to $I_2 =$ constant is

$$r_i = c_1 x^{1/2} \tag{9}$$

for which the factor c_1 is provided by the actual pipe-wall material constraint (8), namely, $c_1 = (3/2)I_2/L^{3/2}$. The pipe that supplies the line of users must become narrower in accelerated fashion as the water approaches the last user ($x = 0$). We return to this aspect of flow architecture in Section 5.

4. Optimal distribution of insulation

We now turn our attention to the optimal spreading of a specified amount of insulating material, Eq. (6). We consider three ways to pursue the optimization:

(i) Maximize the temperature of the hot water received by the most disadvantaged user, the "end" user, the farthest from the source, the one who receives the coldest water,

$$T_0 = T(x = 0). \tag{10}$$

(ii) Minimize the rate of heat leakage from the entire pipe system,

$$q = \int_0^L q'\,\mathrm{d}x. \tag{11}$$

(iii) Maximize the hot-water temperature averaged over all the users,

$$\overline{T} = \frac{1}{L}\int_0^L T\,\mathrm{d}x. \tag{12}$$

For option (i), we obtain an expression for T_0 by setting $x = 0$ in Eq. (4). To maximize T_0 means to minimize the integral that appears in the argument of the exponential on the right side of Eq. (4),

$$I_3 = \int_0^1 \frac{\mathrm{d}\xi}{\xi \ln R}, \tag{13}$$

where

$$\xi = x/L, \qquad R(\xi) = r_0/r_i. \tag{14}$$

The material constraint (6) in combination with the optimized pipe radius (10) means that the integral constraint that must be satisfied by $R(\xi)$ is

$$I_4 = \int_0^1 (R^2 - 1)\xi\,\mathrm{d}\xi, \tag{15}$$

where $I_4 = V/(\pi L^2 c_1^2)$. The function R that minimizes I_3 subject to constant I_4 is obtained implicitly by variational calculus,

$$\xi = c_2/(R \ln R). \tag{16}$$

The factor c_2 is determined by using this R function into the calculation of the actual (specified) amount of insulating material, I_4. Combining Eqs. (15) and (16) we obtain the function $c_2(I_4)$ shown by the solid line in Fig. 2. The factor c_2 is almost proportional to the amount of insulation material, I_4. This makes sense, because c_2 is also proportional to $R \ln R$, cf. Eq. (16): thicker insulations (larger R values) require more insulation material.

According to Eq. (16), the radii ratio $R = r_0/r_i$ increases nearly as $1/\xi$ as the stream approaches the last user ($\xi \to 0$). Since r_i decreases as $\xi^{1/2}$ in the same direction, cf. Eq. (9), the outer radius of the insulation varies nearly as $\xi^{-1/2}$. Furthermore, the integrand of the material constraint (15) shows that in this design the amount of insulation per unit of pipe length increases

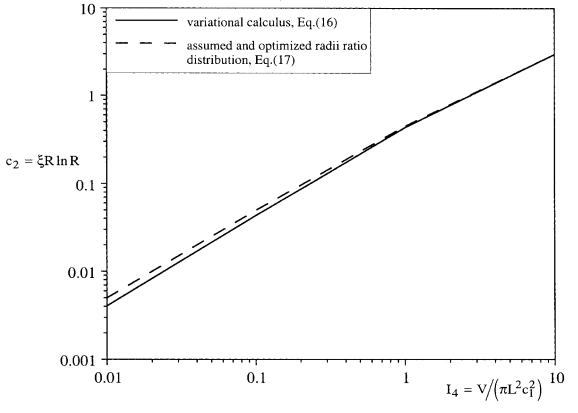

Fig. 2. The effect of the total amount of insulation material (I_4) on the optimal distribution of insulation (c_2).

toward the $\dot{m} = 0$ end of the pipe. This behavior is confirmed by Fig. 3, which shows a plot of Eq. (16) for several amounts of insulation material (I_4).

Finally, the maximized end temperature is obtained by substituting Eq. (16) into I_3 and, finally, into Eq. (4) written for $x = 0$. The chart constructed in Fig. 4(a) shows that the maximized end temperature increases monotonically as the number of heat transfer units of the entire insulation (N) decreases, and as the total amount of insulation (I_4) increases. In summary, Fig. 4 reports the maximized performance of the entire system, as a function of its two global constraints, material and length (or flow residence time).

A more transparent alternative to the variational-calculus route to Figs. 2–4(a), is to go back to Eqs. (13) and (15) and assume that the radii ratio depends on ξ in accordance with

$$\ln R = c_2' \xi^{-n}, \tag{17}$$

where c_2' and n are two constants. By substituting Eq. (17) into Eqs. (13) and (15) we obtain $I_3 = 1/(c_2' n)$ and $I_4 = \text{function}(c_2', n)$. Next, we eliminate c_2' numerically between I_3 and I_4, and the result is $I_3 = \text{function}(n, I_4)$, where I_4 is a constant that accounts for the material constraint. The exponent n accounts for the longitudinal shape (profile) of layer of insulation. In summary, the optimized $R(\xi)$ distribution (17) depends on the amount of material (I_4). This distribution can be expressed numerically in the form of Eq. (16), by recalculating c_2 as a function of I_4, as shown by the dashed line in Fig. 2. The assumed and optimized distribution, Eq. (10), leads to essentially the same insulation geometry as the variational calculus route, Eq. (16).

Next, we determine numerically that I_3 can be minimized with respect to n for a given value of I_4, so that the end temperature is maximized. The optimal exponent $n_{\text{opt}}(I_4)$ is reported in Fig. 4(b). This value can be worked back through the analysis, to deduce the corresponding c_2' value (as plotted in Fig. 4(b)), and the minimized objective integral, $I_{3,\min}$. The latter corresponds to the maximized end temperature of the water stream, which is obtained from Eq. (4): this result was plotted with dashed line in Fig. 4(a), to show that this near-optimal design performs in nearly the same manner as the optimal design deduced based on variational calculus.

The corresponding near-optimal results for the distribution of R versus ξ have been drawn with dashed line in Fig. 3. The optimal and near-optimal insulation profiles are similar: R decreases and tends to 1 as ξ increases. While making this comparison we found that the function $R(\xi, c_2)$ of Eq. (16) is closely approximated by the power-law expression

$$R \cong \left[1 + 1.056(c_2/\xi)^{0.94}\right]^{0.763}. \tag{18}$$

This relation is accurate within 1.2% in the range $0.01 < \xi/c_2 < 100$. The corresponding results for the maximized end temperature of the water stream are shown by dashed curves in Fig. 4(a).

Consider now option (ii), where the objective is the minimization of the rate of heat loss from the entire system. We perform the heat loss integral (11) by using the q' expression (2). The result can be expressed in dimensionless form as

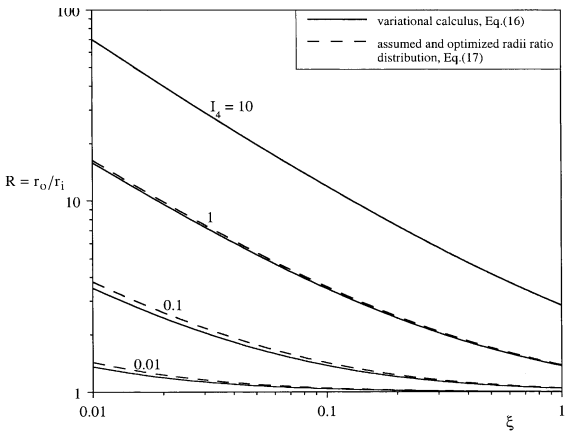

Fig. 3. The optimal ratio of insulation radii when the temperature of the hot water delivered to the farthest user is maximized.

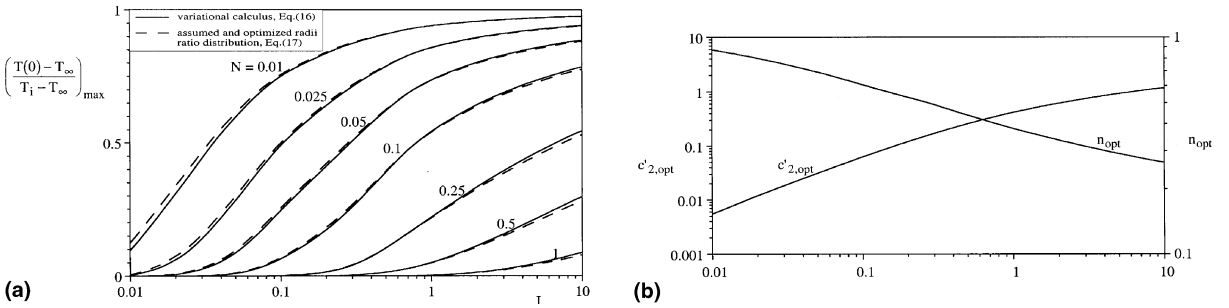

Fig. 4. The maximized and temperature as a function of the amount of insulation material (I_4) and the heat transfer number N, and the optimized constants for the assumed distribution of insulation, Eq. (17).

$$\tilde{q} = \frac{q}{2\pi k(T_i - T_\infty)L} = \int_0^1 \exp\left(-N\int_\xi^1 \frac{d\eta}{\eta \ln[R(\eta)]}\right)\frac{d\xi}{\ln R(\xi)}. \quad (19)$$

Once again, unknown is the insulation radii ratio $R(\xi)$, which must satisfy the insulation material constraint (15). We were not able to optimize $R(\xi)$ based on a variational calculus formulation. Instead, we assumed again functions of the class

$$\ln R = c_3 \xi^n, \quad (20)$$

where c_3 and n are related via the constraint (15), such that the integral (17) expresses the function $\tilde{q}(n,N)$. The method is the same as the one described after Eq. (17). Minimizing $\tilde{q}$ with respect to n we found the radii ratio distribution shown in Fig. 5.

For option (iii), the average water delivery temperature (12) is obtained by averaging the $T(x)$ expression (4),

$$\tilde{T} = \frac{\overline{T} - T_\infty}{T_i - T_\infty} = \int_0^1 \exp\left(-N\int_\xi^1 \frac{d\eta}{\eta \ln[R(\eta)]}\right)d\xi. \quad (21)$$

Using the functions (20) subject to the constraint (15), we derive from the integral (19) the function $\tilde{T}(n,a)$ which can be maximized with respect to n. We find in this way that the optimal distribution of insulation in option (iii) is the same as in option (ii). Both sets of results are represented by dashed lines in Fig. 5. There is little difference between these results and the results based on option (i) – the maximization of end-user water temperature (solid lines in Fig. 5). Consequently, the more complex heat and fluid flow structures optimized in the remainder of the paper are based on option (i).

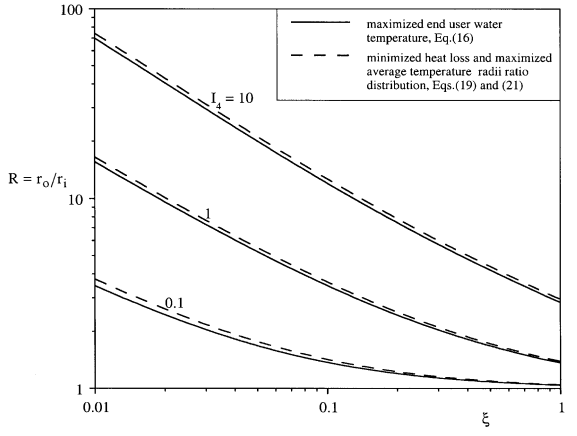

Fig. 5. The optimal ratio of insulation radii when the end user temperature is maximized (solid line), the total heat loss is minimized (dashed line) and the temperature averaged over all the users is maximized (dashed line); $N = 0.01$.

5. Near-optimal pipe radius

The optimal shapes and distributions of insulation derived in Sections 2–4 are useful for orientation. They are based on simplest possible models, and, consequently, they indicate trends and opportunities for optimization in actual engineering applications. The latter demand more realistic models that account not only for objective and constraints, but also for manufacturing realities and the availability of pipe and insulation sizes.

A good example of how the preceding analysis may be adapted to a more realistic model is recommended by the optimal pipe shape derived in Eq. (9). Variational calculus identified a pipe shape characterized by a pipe radius that decreases smoothly all the way to zero at the point where it reaches the last user. The $r_i \to 0$ behavior is certainly unrealistic in pipe systems that must be manufactured, purchased and installed. An alternative is to account from the start for the fact that the smallest pipe size must be *finite*

$$r_i(x = 0) = r_{i0}, \quad \text{finite}. \quad (22)$$

The ensuing analysis continues to have the objective of minimizing the pumping power integral I_1, Eq. (7), subject to the wall material constraint I_2, Eq. (8). The resulting $r_i(x)$ function that minimizes I_1, however, represents a near-optimal design, because the assumed finite-r_{i0} feature is foreign to the truly optimal solution, Eq. (9).

We illustrate this step toward a more realistic model by assuming that the pipe $r_i(x)$ is shaped as the frustum of a cone

$$r_i(x) = r_{i0} + c_4 x. \quad (23)$$

The factor c_4 is dimensionless and represents the slope of the cone generator. Although both r_{i0} and c_4 may vary, they must satisfy the wall material constraint (8), which yields

$$\frac{I_2}{L^2} = \frac{r_{i0}}{L} + \frac{c_4}{2}, \quad \text{constant}. \quad (24)$$

The total pumping power integral (7) becomes

$$I_1 L = \int_0^1 \frac{\xi^3 d\xi}{[(r_{i0}/L) + c_4\xi]^5} = \text{function}\left(\frac{r_{i0}}{L}, c_4\right). \quad (25)$$

By eliminating r_{i0}/L between Eqs. (24) and (25) we obtain $I_1(L)$ as a function of c_4 and the I_2/L^2 constant. This function is then minimized with respect to c_4, and the results are $c_{4,\text{opt}} = 1.2I_2/L^2$ and $I_{1,\min}L = 0.0953(I_2/L^2)^{-5}$. The proportionality between cone angle ($c_{4,\text{opt}}$) and wall material (I_2/L^2) means that in the limit of small ducts ($I_2/L^2 \to 0$) the optimal cone frustum approaches a pipe of constant radius. In agreement with expectations, the minimized pumping power ($I_{1,\min}L$) increases sharply as the pipe size decreases ($I_2/L^2 \to 0$). It can be verified

that these trends match quantitatively the trends exhibited by the variational calculus solution in Section 3.

6. Users distributed uniformly over an area

In this section we turn our attention to the more important and practical question of how to distribute a hot-water stream to a population of users spread over an area, A. One solution is to coil the optimized string of users in such a way that the area is covered. Two possibilities are sketched in the lower part of Fig. 1. The string of length L and width L_0 can cover a disk-shaped area of diameter $D = [(4/\pi)L_0L]^{1/2}$, or a square-shaped area of side $S = (L_0L)^{1/2}$. Are these the best ways to allocate the hot water stream to the entire area?

The alternative is to introduce branches in the path of the stream, and to distribute area elements to each branch. We explore this alternative by starting with the smallest (and therefore simplest) area element, and continuing toward larger areas by assembling elements into larger and larger constructs. One simple rule of assembly is to use four constructs into the next, larger assembly, Fig. 6. In this case each construct covers a square area, in the sequence $A_0 = L_0^2$, $A_1 = 4L_0^2$, $A_2 = 4^2L_0^2, \ldots, A_i = 4^iL_0^2$. This assembly rule is 'simple' because the shape (square) of each construct is assumed, not optimized. An alternative construction sequence is described in Section 7.

The objective is to supply with hot water the users distributed uniformly over A_i, and to accomplish this task with minimal pumping power and a finite amount of thermal insulation. The geometry of each pipe is described by its length (a fraction or multiple of L_0), inner radius wetted by the flow (r_i), and ratio of insulation radii ($R = r_0/r_i$). The pipe wall thickness is neglected for the sake of simplicity. The subscripts 0, 1 and 2, indicate the elemental area, first construct, and second construct, in accordance with the notation shown in Fig. 6.

To minimize the pumping power requirement at the elemental level ($\dot{W}_0 = \dot{m}_0\Delta P_0/\rho$) is to minimize the pressure drop along the elemental duct of the length $L_0/2$. Assuming as in the earlier sections that the flow is fully-developed turbulent in the fully rough regime (f = constant), we find that the pressure drop derived from the definition of friction factor [2,24] is

$$\Delta P_0 = \frac{f}{\pi^2}\frac{\dot{m}_0^2 L_0/2}{\rho r_{i0}^5}. \tag{26}$$

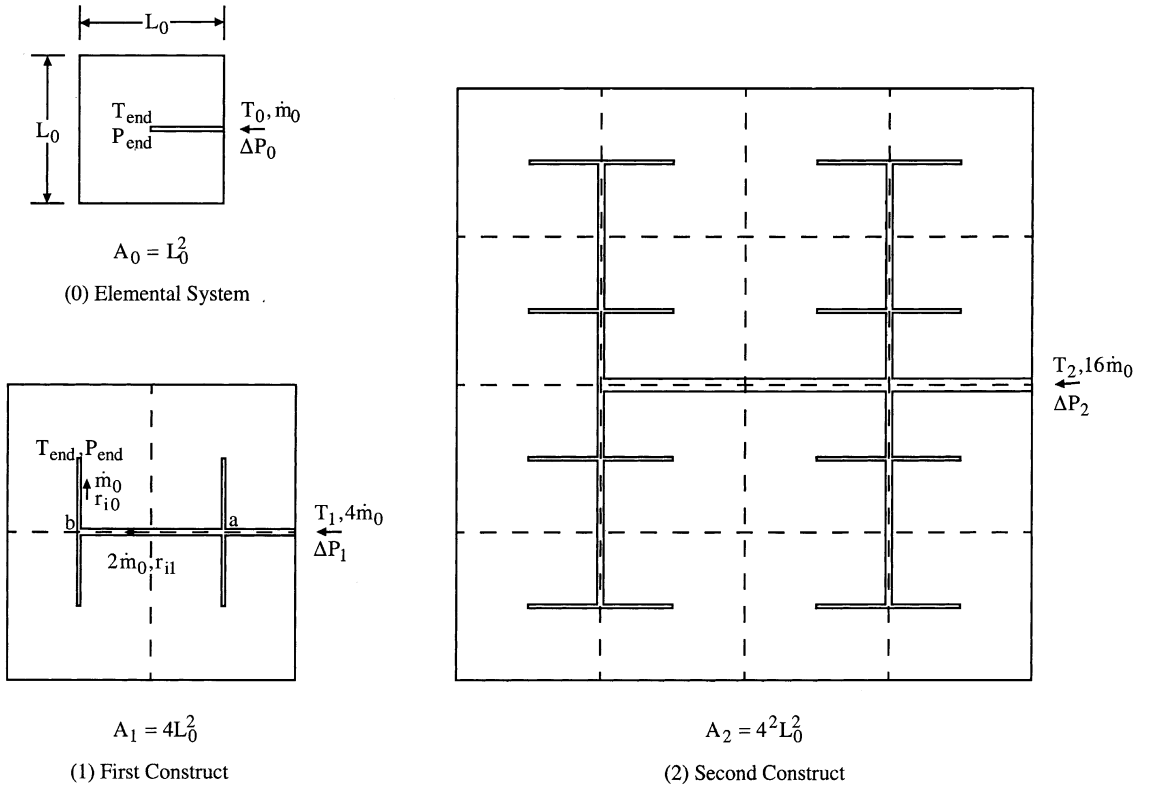

Fig. 6. Sequence of square-shaped constructs containing tree-shaped streams of hot water.

The corresponding heat-loss analysis based on Eq. (3), with $\dot{m}_0 =$ constant in place of $\dot{m}$, yields the temperature drop from the inlet to the element (T_0) to the user (T_{end})

$$\frac{T_{\text{end}} - T_\infty}{T_0 - T_\infty} = \exp\left(-\frac{N_0}{\ln R_0}\right), \tag{27}$$

where the number of heat loss units is based on elemental quantities

$$N_0 = \frac{\pi k L_0}{\dot{m}_0 c_{\text{p}}}. \tag{28}$$

At the first-construct level there are two pipe sizes, one central pipe of length $(3/2)L_0$ and radii $r_{\text{i}1}$ and $R_1 = (r_0/r_{\text{i}})_1$, and four elemental branches of length $(1/2)L_0$ and radii $r_{\text{i}0}$ and $R_0 = (r_0/r_{\text{i}})_0$. The flow rate is $4\dot{m}_0$ through the root of the tree, and $\dot{m}_0$ through each small branch. By writing the equivalent of Eq. (26) for each segment of pipe without branches, we find that the drop in pressure from the root to the most distant user (the center of the farthest element) is

$$\Delta P_1 = \frac{f}{\pi^2}\frac{\dot{m}_0^2 L_0}{\rho}\left(\frac{12}{r_{\text{i}1}^5} + \frac{1}{2r_{\text{i}0}^5}\right). \tag{29}$$

By analogy with the shaping of the water duct volume in Section 3, the pressure drop ΔP_1 can be minimized by selecting the ratio of pipe sizes $r_{\text{i}1}/r_{\text{i}0}$ subject to a water volume constraint. If, as in Section 3, we constrain the amount of duct wall material, and if we assume that the duct thickness (t) is a constant independent of duct inner radius, then the constraint means that the total wetted surface is fixed

$$\frac{3}{2}L_0 r_{\text{i}1} + 2L_0 r_{\text{i}0} = \text{constant}. \tag{30}$$

The same geometric relation applies when the constraint refers to the amount of soil that must be excavated in order to bury the pipe system to a constant depth. The minimization of ΔP_1 subject to constraint (30) yields

$$(r_{\text{i}1}/r_{\text{i}0})_{\text{opt}} = 2^{5/6}. \tag{31}$$

An alternative is to fix the total volume occupied by the ducts

$$\frac{3}{2}L_0 r_{\text{i}1}^2 + 2L_0 r_{\text{i}0}^2 = \text{constant}. \tag{32}$$

This constraint also represents applications where the thickness of each pipe is proportional to the pipe inner radius, and where the total amount of wall material is constrained. In such cases, the minimization of ΔP_1 subject to constraint (32) yields a slightly different optimal step in pipe size

$$(r_{\text{i}1}/r_{\text{i}0})_{\text{opt}} = 2^{5/7}. \tag{33}$$

The optimization of the geometry of the thermal insulation shells wrapped around each pipe proceeds in the same steps as the pressure-drop minimization. We write a temperature drop expression of type (27) for each segment of pipe without branches. We omit the algebra and report only the overall temperature drop from the root of the tree (T_1) to the temperature (T_{end}) of the water stream delivered to the most distant user

$$\theta_1 = \frac{T_{\text{end}} - T_\infty}{T_1 - T_\infty} = \exp\left(-\frac{N_0}{\ln R_0} - \frac{5N_0}{4\ln R_1}\right). \tag{34}$$

The dimensionless end temperature θ_1 depends on three parameters, R_0, R_1 and N_0. The geometric parameters R_0 and R_1 are related through the thermal insulation volume constraint

$$V_1 = \pi L_0 r_{\text{i}0}^2\left[\frac{3}{2}\left(\frac{r_{\text{i}1}}{r_{\text{i}0}}\right)^2\left(R_1^2 - 1\right) + 2\left(R_0^2 - 1\right)\right] \tag{35}$$

for which $(r_{\text{i}1}/r_{\text{i}0})$ is a number furnished by Eq. (31) or Eq. (33). Constraint (35) may be put into the dimensionless form $\tilde{V}_1(R_0, R_1)$ by recognizing $r_{\text{i}0}$ as the smallest pipe size (Section 5) and defining the dimensionless insulation volume $\tilde{V}_1 = V_1/\left(\pi r_{\text{i}0}^2 L_0\right)$.

The maximization of expression (34) with respect to R_0 and R_1, and subject to constraint (35) yields the optimal step change in radii ratio

$$\left(\frac{R_1 \ln R_1}{R_0 \ln R_0}\right)_{\text{opt}} = \left(\frac{5}{6}\right)^{1/2}\left(\frac{r_{\text{i}0}}{r_{\text{i}1}}\right)_{\text{opt}}. \tag{36}$$

In view of the $(r_{\text{i}1}/r_{\text{i}0})_{\text{opt}}$ values listed in Eqs. (31) and (33), we conclude that $R_{1,\text{opt}} < R_{0,\text{opt}}$, i.e., the shell of the central duct is relatively thin in comparison with the shells of the elemental ducts. Relatively 'thin' means that the shell thickness is small in comparison with the radius of the same tube. Combining the function $R_{1,\text{opt}}(R_{0,\text{opt}})$ of Eq. (36) with the $\tilde{V}_1(R_0, R_1)$ constraint (35) we obtain the radii ratios $R_{0,\text{opt}}(\tilde{V}_1)$ and $\tilde{R}_{1,\text{opt}}(\tilde{V}_1)$ displayed in Fig. 7(a). The same figure shows the evolution of the step change in geometric form, $(R_1/R_0)_{\text{opt}}$, as the amount of insulation $\tilde{V}_1$ increases. Noteworthy is that the optimized architecture of the distributed insulation is independent of N_0. Once again, the value of $(r_{\text{i}1}/r_{\text{i}0})_{\text{opt}}$, or the choice between constraints (30) and (32) has little effect on the insulation geometry.

The maximized performance of the first construct is measured by the θ_1 values obtained by substituting into Eq. (34) the optimized geometry reported in Fig. 7(a). The result is the function $\theta_{1,\max}(N_0, \tilde{V}_1)$ presented in Fig. 7(b). The temperature of the water stream delivered to the farthest user increases as the amount of insulation increases, and as the thermal conductivity of the insulating material (N_0) decreases. These trends agree with what we saw in Fig. 4(a) following the optimization of the distribution of insulation in the string-shaped system, Fig. 1.

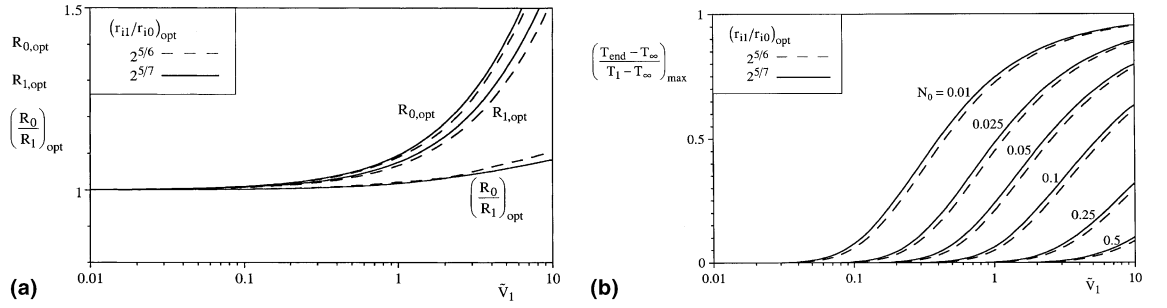

Fig. 7. The optimal ratios of insulation radii for the first construct (A_1) shown in Fig. 6, and the maximized end temperature of the first construct.

The optimization of the internal architecture of the second construct (A_2, Fig. 6) is performed by executing the same steps as in the optimization of the first construct. New is the larger size of the construct ($A_2 = 4A_1, \dot{m}_2 = 16\dot{m}_0$) and the new central duct of length $3L_0$, inner radius r_{i2} and insulation radii ratio $R_2 = r_{o2}/r_{i2}$. The optimized geometric features of the first construct are retained.

In the fluid flow part of the problem we minimize the overall pressure drop from the root of the fluid tree (P_2) to the farthest user (P_{end}), namely $\Delta P_2 = P_2 - P_{end}$. After some algebra we obtain

$$\Delta P_2 = \frac{f}{\pi^2}\frac{\dot{m}_2^2 L_0}{\rho}\left(\frac{3/2}{r_{i2}^5} + \frac{12+\beta^{5/2}}{16^2 r_{i1}^5}\right), \tag{37}$$

where $\beta = (r_{i1}/r_{i0})^2$ is shorthand for a numerical value provided by Eq. (31) or Eq. (33). Recall that at the first-construct level we used two alternative water-space constraints, Eqs. (30) and (32), and the geometric optimization results were quite similar, cf. Figs. 7(a) and (b). For this reason we continue only with the constraint of type (32) in which we fix the volume of all the ducts of the A_2 construct, namely $\pi L_0\left[3r_{i2}^2 + r_{i1}^2(6+8/\beta)\right] = \text{constant}$. By varying r_{i2} and r_{i1} subject to this constant, we minimize ΔP_2 and find the optimal relative size of the central duct of the A_2 construct

$$\left(\frac{r_{i2}}{r_{i1}}\right)_{opt} = \left(\frac{3+4/\beta}{24+\beta^{5/2}}\cdot 2^9\right)^{1/7} = 2^{6/7}. \tag{38}$$

Noteworthy is the inequality $(r_{i2}/r_{i1})_{opt} > (r_{i1}/r_{i0})_{opt}$, which states that the step change in duct size is more abrupt at the second-construct level than at the first-construct level.

The second part of the analysis of A_2 is concerned with the temperature (T_{end}) of the water stream received by the farthest elemental user, and the maximization of this temperature subject to the constrained total volume of thermal insulation allocated to the A_2 construct. The analysis yields an expression for the dimensionless overall temperature drop

$$\theta_2 = \frac{T_{end}-T_\infty}{T_2-T_\infty} = \theta_1 \exp\left(-\frac{5N_0/8}{\ln R_2}\right), \tag{39}$$

where $\theta_1(N_0, \tilde{V}_1)$ is a function that is available numerically based on the optimization of the A_1 construct (cf. Fig. 7(b)). The total insulation volume (V_2) constraint for the A_2 construct can be written as

$$\tilde{V}_2 = \frac{V_2}{\pi r_{i0}^2 L_0} = 3\left(\frac{r_{i2}}{r_{i0}}\right)^2\left(R_2^2 - 1\right) + 4\tilde{V}_1, \tag{40}$$

where r_{i2}/r_{i0} is a numerical factor known from the minimization of pressure, for example $r_{i2}/r_{i0} = (r_{i2}/r_{i1})$

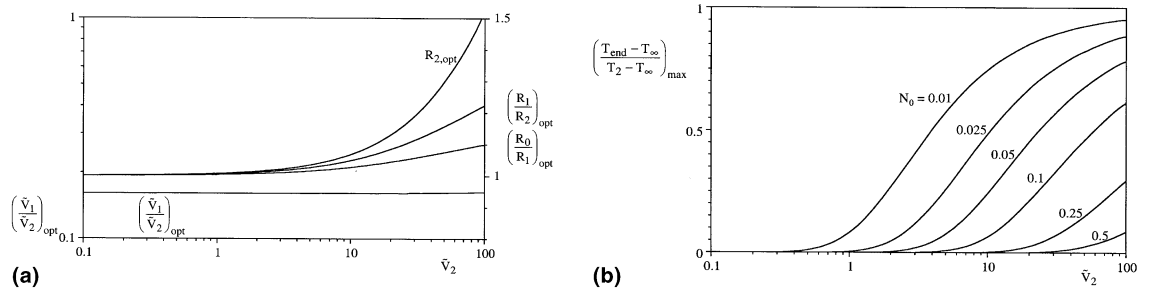

Fig. 8. The optimal ratios of insulation radii for the second construct (A_2) shown in Fig. 6, and the maximized end temperature of the second construct.

$(r_{i1}/r_{i0}) = 2^{11/7}$ if the water-space constraint used is the total volume of the ducts.

In summary, the end-temperature function $\theta_2(N_0, \tilde{V}_1, R_2)$ of Eq. (39) and the constraint $\tilde{V}_2(\tilde{V}_1, R_2)$ of Eq. (40) define θ_2 as a function of $N_0, \tilde{V}_2$ and R_2. By maximizing θ_2 with respect to R_2 at constant N_0 and $\tilde{V}_2$ we obtain the insulation radii ratio $R_{2,\mathrm{opt}}$ and maximized end temperature reported in Figs. 8(a) and (b).

The relative superiority of the tree-shaped design (Fig. 6) over the string design (Fig. 1) is documented in Fig. 9. Here we show the dimensionless end temperatures produced by the two optimized schemes on the same basis – the same covered territory (A_2) and the same amount of insulation used in the entire construct (V_2). It is clear that the tree-shaped design is superior, as the end-user water temperature in the scheme of Fig. 6 is consistently higher than in the coiled string arrangement of Fig. 1. The two schemes have nearly the same performance in the limit of plentiful insulation material ($\tilde{V}_2 > 10^2$) and high water flow rate ($N_0 < 10^{-2}$).

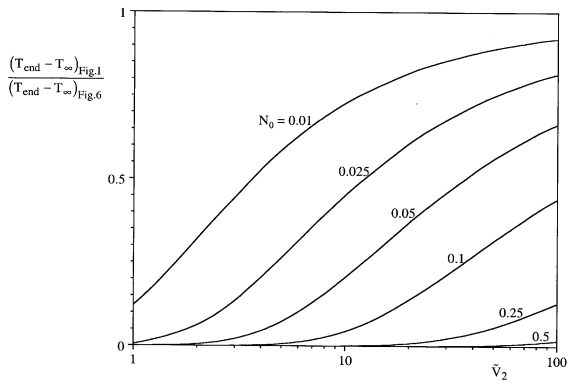

Fig. 9. Comparison between the maximized water stream temperatures delivered to the farthest users in the string-shaped construct of Fig. 1 and the tree-shaped first construct (A_2) of Fig. 6, for the same territory covered by the construct, and the same total amount of insulation.

7. Tree network generated by repetitive pairing

The sequence of square-shaped constructs used beginning with Fig. 6 is an assumption, not a result of optimization. To see whether a better rule of assembling small constructs into larger constructs can be found, consider the area doubling sequence shown in Fig. 10. Each area construct is obtained by putting together two constructs of the immediately smaller size. The area supplied with hot water increases in the sequence $A_0 = L_0^2, A_1 = 2L_0^2, A_2 = 2^2L_0^2, \ldots, A_i = 2^iL_0^2$, and the shape of the area alternates between square and rectangular. The elemental area that starts the sequence in Fig. 10 is the same as in Fig. 6, namely A_0. The second construct of Fig. 14 covers the same area ($4L_0^2$) as the first construct of Fig. 6. One objective of the optimization work reported in this section is to see which area construction sequence serves the farthest (end) user of the $4L_0^2$ territory better, Fig. 6 or Fig. 10?

For the sake of brevity, we report only the results of the minimization of water flow resistance and loss of heat to the ambient. The analysis follows step-by-step the analysis detailed in the preceding section. For the first construct of Fig. 10, in place of Eqs. (31) and (33) we obtain

$$(r_{i1}/r_{i0})_{\mathrm{opt}} = 2^{1/2}, \tag{41}$$

$$(r_{i1}/r_{i0})_{\mathrm{opt}} = 2^{3/7}, \tag{42}$$

which correspond to invoking the duct wall material and, respectively, duct volume constraints. Eqs. (34) and (35) are replaced by

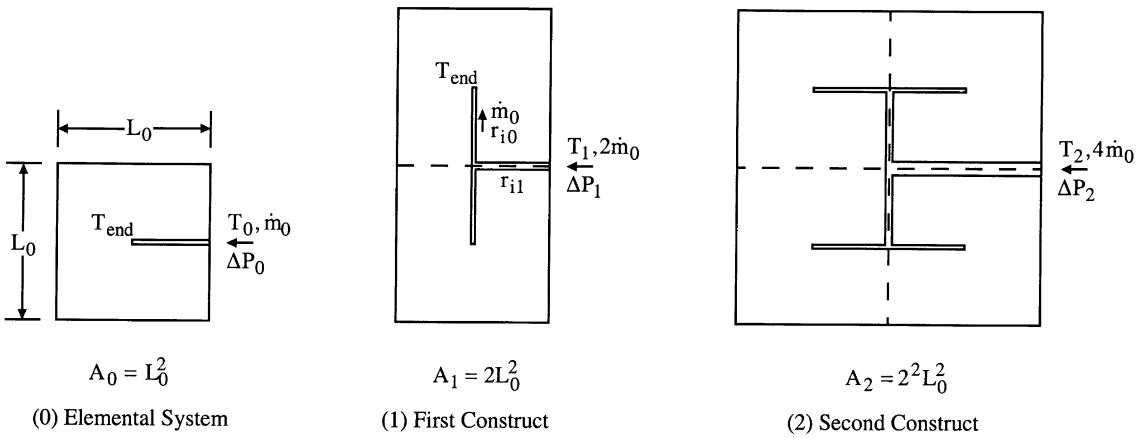

Fig. 10. Sequence of area constructs obtained by pairing smaller constructs.

$$\theta_1 = \frac{T_{\text{end}} - T_\infty}{T_1 - T_\infty} = \exp\left(-\frac{N_0}{\ln R_0} - \frac{N_0}{2\ln R_1} \right), \tag{43}$$

$$\tilde{V}_1 = \frac{V_1}{\pi L_0 r_{\text{i}0}^2} = \frac{1}{2}\left(\frac{r_{\text{i}1}}{r_{\text{i}0}}\right)^2 (R_1^2 - 1) + (R_0^2 - 1). \tag{44}$$

The results for the optimal distribution of insulation and maximized end-user water temperature are reported in Figs. 11(a) and (b). The choice of constraint, i.e., Eq. (41) vs Eq. (42), has a small effect, therefore we proceed by using only the duct volume constraint.

At the second-construct level, in place of Eq. (38) we obtain $(r_{\text{i}2}/r_{\text{i}1})_{\text{opt}} = 2^{3/7}$. The user temperature and total insulation volume are

$$\theta_2 = \frac{T_{\text{end}} - T_\infty}{T_2 - T_\infty} = \theta_1 \exp\left(-\frac{N_0}{2\ln R_2} \right), \tag{45}$$

$$\tilde{V}_2 = \frac{V_2}{\pi L_0 r_{\text{i}0}^2} = \left(\frac{r_{\text{i}2}}{r_{\text{i}0}}\right)^2 (R_2^2 - 1) + 2\tilde{V}_1. \tag{46}$$

The optimal distribution of the finite amount of insulation is reported in Fig. 12(a), and the maximized user water temperature in Fig. 12(b).

The numerical values and trends are similar to what we saw earlier. More to the point, we can compare the relative goodness of the doubling sequence (Fig. 10) vs the sequence of square areas (Fig. 6). In Fig. 13 we show the ratio of the maximized end temperatures of Figs. 7(b) and 12(b), with the observation that both figures refer to the same construct size ($4L_0^2$), and that the insulation volume V_1 of Fig. 7(b) is set equal to V_2 of Fig. 12(b). The total duct volume is the same in the two designs sketched above the graph. Note also that $r_{\text{i}0}$ of Fig. 7(b) is not the same as the $r_{\text{i}0}$ of Fig. 12(b), and, consequently, the dimensionless volumes $\tilde{V}_{1,\text{Fig. 7(b)}}$ and $\tilde{V}_{1,\text{Fig. 12(b)}}$ are not the same. The comparison shown in Fig. 13 allows us to conclude that the tree structure generated by repeated pairing (A_2, Fig. 10) is superior to the square structure (A_1, Fig. 6). The temperature of the hot water received by the end user in Fig. 10 (A_2) is consistently higher. The trends and the domain in which the two schemes perform at nearly the same level are similar to what we saw in the comparison between the square tree and the coiled string designs in Fig. 9.

We pursued this comparison to an even higher level of assembly – the construct of size $16L_0^2$ – on the basis of the same mount of insulation material and total duct volume. The two structures are illustrated in the upper part of Fig. 14, with the observation that the tree generated by repeated pairing (A_4) is not shown in Fig. 10. Once again, the tree design based on the sequence of

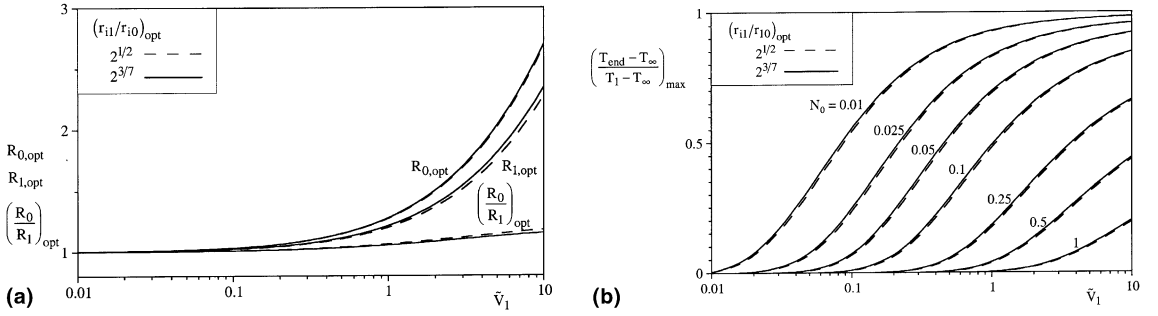

Fig. 11. The optimal ratios of insulation radii for the first construct (A_1) shown in Fig. 10, and the maximized end temperature of the first construct.

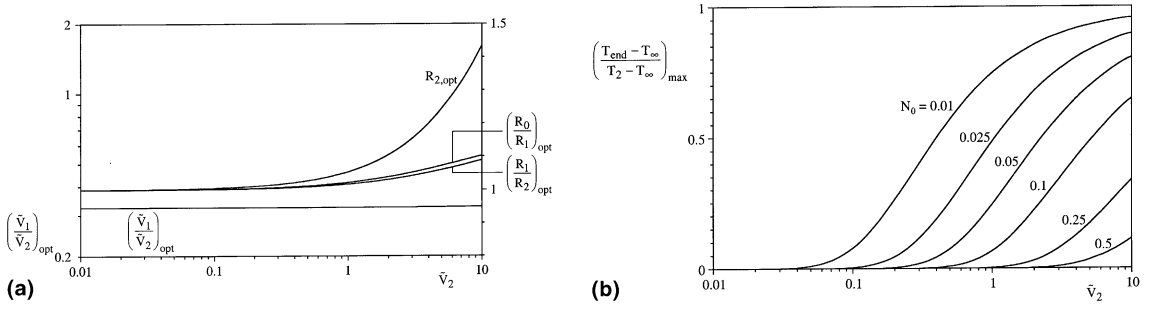

Fig. 12. The optimal ratios of insulation radii for the second construct (A_2) shown in Fig. 10, and the maximized end temperature of the second construct.

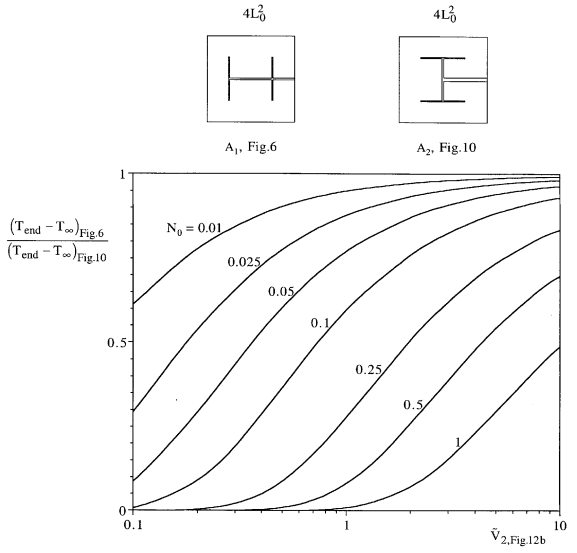

Fig. 13. Comparison between the maximized end-user water temperature on the $4L_0^2$ construct, according to the construction sequences of Figs. 6 and 10.

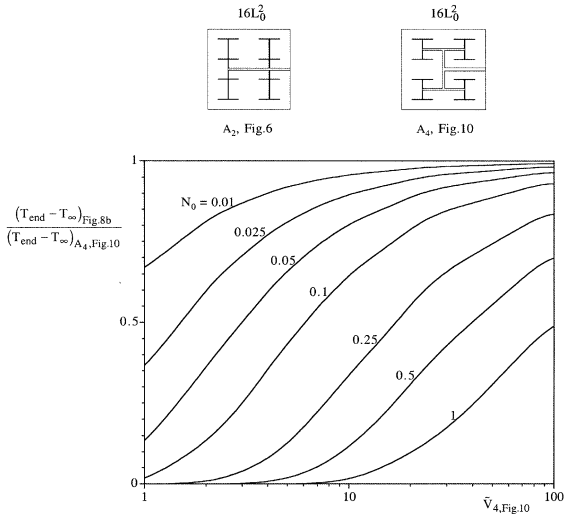

Fig. 14. Comparison between the maximized end-user water temperature on the $16L_0^2$ construct, according to the construction sequences of Figs. 6 and 10.

Fig. 10 outperforms the design based on Fig. 6. By comparing Figs. 14 and 13 on the same basis (the same L_0, total pipe volume, total amount of insulation), it can be shown that the difference in the global performance of the two types of trees (Fig. 6 and Fig. 10) diminishes as each optimized tree structure becomes more complex. The global performance becomes progressively less sensitive to the actual layout of the tubes, provided that the distributions of tube step sizes and shells of insulation material have been optimized. When the optimized tree structure becomes more complex it also becomes more robust with respect to changes in the tree pattern.

It is worth pointing out another useful property of the pairing sequence (Fig. 10): each user receives hot water at the same temperature. The $\dot{m}_0$ stream received by each user passes through the same sequence of insulated tubes. This is a very useful property, because in other tree structures such as Fig. 6, the users located closer to the root of the tree receive warmer streams than the farther users. The tree designs of Fig. 10 deliver hot water to the territory uniformly – uniformly in space and in temperature.

We verified these conclusions by constructing Figs. 13 and 14 in an alternative way. The first way was to assemble each construct (e.g. $4L_0^2$ in Fig. 13) by putting together previously optimized smaller systems (constituents). In this way the optimized features determined for the smaller areas were preserved in the larger construct. The alternative was to begin with the needed (large) construct, and to let all the geometric parameters vary freely. Along this route, we optimized every geometric feature and arrived at exactly the same final structure as during the first approach. These alternative calculations of the optimized structures compared in Figs 13 and 14 verify the accuracy of the results presented in these figures.

8. Concluding remarks

In this paper, we treated in some detail the basic problem of distributing hot water to users spread over a territory, when the amount of insulation and other constraints are in place. The optimal distribution of insulation over the many pipes of the network was necessary step, but not the main focus of this study. The main focus was on the topology of the water distribution network – the layout of the pipes over the territory. Main questions were how the layout can be deduced from the objective of maximizing the global performance of the hot water distribution system, and to what extent the choice of layout influences global performance.

In the first part of the study (Sections 2–5) we established the method of analysis and optimization, by starting with the simplest arrangement: a string of water users attached to a single stream (Fig. 1). We maximized the system performance in three ways (review options (i)–(iii), Section 4), and found that the geometry of the optimally distributed insulation material is practically insensitive to the optimization criterion used (Fig. 5). Along the way we showed that more accessible methods of analysis (e.g., Eq. (17)) yield nearly the same results as the method of varitional calculus. More realistic features can be added to the model, as we demonstrated by

introducing as constraint the smallest pipe size that is available (Section 5).

The second part of the paper dealt with the spreading of the hot water distribution system over a two-dimensional territory. Here we used the constructal sequence [1] of optimizing smaller systems, and assembling them into progressively larger systems (Figs. 6 and 10). In each tree structure we optimized the distribution of insulation by maximizing the temperature of the water received by the farthest user. We found that the designs generated by the construction sequence in which each structure contains two structures of the preceding size (Fig. 10) perform consistently better than the designs produced by the sequence of squares (Fig. 6). In addition, the designs generated according to Fig. 10 are superior because they deliver water at the same temperature to all the users.

The difference in performance between one type of tree structure over another decreases as the complexity of the structure increases. It is as if "any tree will do" if it is large and complex enough, and if its link dimensions and insulation have been optimized. Tree-shaped distribution systems perform consistently and substantially better than string-shaped or coil-shaped systems (Fig. 9). The robustness of the tree-flow performance to differences in internal layout (Fig. 6 vs Fig. 10) is important because it simplifies the search for a nearly-optimal layout, and because a constructed system will function at near-optimal levels when its operating conditions drift from the values for which the system was optimized.

The chief conclusion of this study is that the use of geometric form (shape, structure) is an effective route to achieving high levels of global performance under constraints. The brute force approach of delivering hot water by using large amounts of insulation and flow rate (small N) is not economical. Much faster progress toward the goal of global performance maximization can be made by recognizing and treating the topology of the flow system as the main unknown of the problem.

Acknowledgements

This work was supported by a grant from the National Science Foundation. Mr. W. Wechsatol also acknowledges the support received from King Mongkut's University of Technology (KMUTT), Thailand.

References

[1] A. Bejan, Shape and Structure, from Engineering to Nature, Cambridge University Press, Cambridge, UK, 2000.
[2] J. Padet, Fluids en Écoulement Méthodes et Modéles, Masson, Paris, 1991.
[3] A. Dupont, Hydraulique Urbaine, Ouvrages de Transport, Elévation et Distribution, Eyrolles, Paris, 1977.
[4] J. Bonnin, Hydraulique Urbaine Appliqué aux Agglomérations de Petite et Moyenne Importance, Eyrolles, Paris, 1977.
[5] P. Nonclercq, Hydraulique Urbaine Appliquée, CEBEDOC, Liége, 1982.
[6] M. Falempe, Une plate-forme d'enseignement et de recherche du procédé de cogénération chaleur-force par voie de vapeur d'eau, Revue Générale de Thermique 383 (1993) 642–651.
[7] M. Falempe, B. Baudoin, Comparaison des dix méthodes de résolution des réseaux de fluides á usages énergétiques, Revue Générale de Thermique 384 (1993) 669–684.
[8] A. Barreau, J. Moret-Bailly, Présentation de deux méthodes d'optimisation de réseaux de transport d'eau chaude á grande distance, Entropie 75 (1977) 21–28.
[9] B. Plaige, Le chauffage urbain en Pologne Chauffage Ventilation, Condittionement d'Air 9 (1999) 19–23.
[10] W.J. Wepfer, R.A. Gaggioli, E.F. Obert, Economic sizing of steam piping and insulation, J. Eng. Industry 101 (1979) 427–433.
[11] A. Bejan, G. Tsatsaronis, M. Moran, Thermal Design and Optimization, Wiley, New York, 1996.
[12] D'.A.W. Thompson, On Growth and Form, Cambridge University Press, Cambridge, UK, 1942.
[13] D.L. Cohn, Optimal systems: I. The vascular system, Bull. Math. Biophys. 16 (1954) 59–74.
[14] A.L. Bloom, Geomorphology, Prentice-Hall, Englewood Cliffs, NJ, 1978.
[15] E.R. Weibel, Morphometry of the Human Lung, Academic Press, New York.
[16] N. MacDonald, Trees and Networks in Biological Models, Wiley, Chichester, UK, 1983.
[17] L.B. Leopold, M.G. Wolman, J.P. Miller, Fluvial Processes in Geomorphology, Freeman, San Francisco, CA, 1964.
[18] A.E. Scheidegger, Theoretical Geomorphology, 2nd ed., Springer, Berlin, 1970.
[19] R.J. Chorley, S.A. Schumm, D.E. Sugden, Geomorphology, Methuen, London, 1984.
[20] M. Morisawa, Rivers. Form and Process, Longman, London, 1985.
[21] T.A. Wilson, Design of the bronchial tree, Nature 213 (1967) 668–669.
[22] I. Rodriguez-Iturbe, A. Rinaldo, Fractal River Basins, Cambridge University Press, Cambridge, UK, 1997.
[23] P. Meakin, Fractals, Scaling and Growth Far from Equilibrium, Cambridge University Press, Cambridge, UK, 1998.
[24] A. Bejan, Heat Transfer, Wiley, New York, 1993.
[25] F.B. Hildebrand, Advanced Calculus for Applications, Prentice-Hall, Englewood Cliffs, NJ, 1962.